We are IntechOpen, the world's leading publisher of Open Access books Built by scientists, for scientists

6,900
Open access books available

185,000
International authors and editors

200M
Downloads

Our authors are among the

154
Countries delivered to

TOP 1%
most cited scientists

12.2%
Contributors from top 500 universities

WEB OF SCIENCE™

Selection of our books indexed in the Book Citation Index in Web of Science™ Core Collection (BKCI)

Interested in publishing with us?
Contact book.department@intechopen.com

Numbers displayed above are based on latest data collected.
For more information visit www.intechopen.com

11

Quartz Crystal Microbalance in Clinical Application

Ming-Hui Yang[1], Shiang-Bin Jong[2,3], Tze-Wen Chung[1], Ying-Fong Huang[2,3] and Yu-Chang Tyan[2,4,5]
[1]*Department of Chemical and Material Engineering, National Yulin University of Science and Technology*
[2]*Department of Medical Imaging and Radiological Sciences, Kaohsiung Medical University*
[3]*Department of Nuclear Medicine, Kaohsiung Medical University Chung-Ho Memorial Hospital*
[4]*National Sun Yat-Sen University - Kaohsiung Medical University Joint Research Center*
[5]*Center for Resources, Research and Development, Kaohsiung Medical University*
Taiwan

1. Introduction

Human serum albumin (HSA), with a molecular weight of approximately 67 kDa, is a negative acute-phase protein and is the most abundant and characteristic globular unglycosylated serum protein. It is predominantly synthesized in the liver and mainly plays a role in mediating blood volume and regulated by the colloid osmotic pressure (COP) of interstitial fluid bathing the hepatocyte (West, 1990; Peters, 1996). HSA plays an important physiological role as a transporter for various substances. It has a good binding capacity for water, metals (Ca^{2+}, Na^{+}, $K^{+)}$, fatty acids, hormones, bilirubin, ligands, therapeutic drugs and metabolites (Prinsen & de Sain-van der Velden, 2004). In plasma, albumin was comprised about 50% of total plasma protein. This implies that 10-15 g of albumin is produced per day in healthy subjects, which is about 0.4 mg albumin per gram liver per hour. The high steady-state concentration in plasma is 30 to 50 mg/mL (Ballmer et al., 1990). The albumin is minimal urinary loss in healthy subjects. Around 70 kg of albumin that passes through the kidneys each day, only a few grams pass through the glomerular membrane. Nearly all of this is reabsorbed, and urinary loss is usually no more than 10–20 mg per day. Therefore, HSA level in plasma is confirmed to be as a reliable indicator for the prognosis and severity of several diseases, such as liver disease, renal function, infectious disease, and cancer. Hypoalbuminemia, lack of albumin, results from liver disease, over excretion from kidney, excess loss in gastrointestinal system, burns, acute disease, drug effect or malnutrition. Hyperalbuminemia is a sign of serve dehydration or maybe result from the retinol deficiency that all-trans retinoic acid moderate HSA (Rothschild et al., 1988; Moshage et al., 1987; Mariani et al., 1976; Chlebowski et al., 1989; Phillips et al., 1989; Gross et al., 2005).

Self-assembled monolayers (SAMs) have received a great deal of attention for their fascinating potential technical applications such as nonlinear optics and device patterning (Horne & Blanchard, 1998; Morhard et al., 1997; Bierbaum et al., 1995). They also have been used as an ideal model to investigate the effects of intermolecular interactions in the molecular assembly systems (Schertel et al., 1995; Yan et al., 2000; Himmel et al., 1997; Jung et al., 1998). SAMs have been traditionally prepared by immersing a substrate into a solution containing a ligand that is reactive to the substrate surface or by exposing the substrate to the vapor of the reactive species. The most common utilization of the SAMs system is the application of alkanethiolates (AT) on gold (Au), rather than other metals such as platinum, copper, or silver, because gold does not have stable oxide compounds and easily forms a bond with sulfur. The AT SAMs not only provides an excellent model system to study fundamental aspects of surface properties such as wetting (Laibinis et al., 1992) and tribology (Joyce et al., 1992), but also is a promising candidate for potential applications in the fields of biosensors (Gooding &Hibbert, 1999), biomimetics (Erdelen et al., 1994) and corrosion inhibition (Laibinis & Whitesides, 1992).

The quartz crystal microbalance (QCM) with an A-T cut quartz slide equipped with electrodes has been used in various fields, such as environmental protection, chemical technology, medicine, food analysis, and biotechnology (King, 1964; Guilbault, 1983; Guilbault et al., 1988; Guilbault & Luong, 1988; Guilbault et al., 1992; Fawcett et al., 1988). It has been widely used for substance measurement in liquid environments. Previously, research has revealed that measurements in liquid environments are very complicated. Several variations in liquid environments, such as characteristics of crystals and factors of surface interactions, should be controlled and calibrated with accurate and precise machines and mathematical formulas (Attli & Suleman, 1996; Nie et al., 1992; Muramatsu et al., 1988; Voinova et al., 2002). Besides, the amount of sample used in aqueous environments often requires more than can be acquired for analysis from the human body and may be a limitation for use as a clinical immunosensor. The detection theory for QCM can be explained by the Sauerbrey equation, which calculates that the mass change is proportional to the oscillation frequency shift of the piezoelectric quartz crystal (O'Sullivan & Guilbault, 1999). Equation 1 shows the Sauerbrey equation in gas phase. ΔF: the frequency shift (Hz); F: basic oscillation frequency of piezoelectric quartz (Hz); A: the active area of QCM (cm^2); ΔM: the mass change on QCM (g).

$$\Delta F = -2.3 \times 10^{-6} \frac{F^2 \Delta M}{A} \quad (1)$$

This experiment completes a study for a potential biomedical application of functionalized SAMs with the immobilized anti-HSA monoclonal antibody, and a QCM system using the SAMs chip for HSA quantification. The attachment of anti-HSA monoclonal antibody to a SAMs surface was achieved using water soluble N-ethyl-N'-(3-dimethylaminopropyl) carbodiimide hydrochloride (EDC) and *N*-hydroxysuccinimide (NHS) as coupling agents. Surface analyses were utilized by Atomic force microscopy (AFM), X-ray photoelectron spectroscopy (XPS) and Fourier-transformed infrared reflection-reflectance absorbance spectroscopes (FTIR-RAS). The quantization of immobilized antibody was characterized by the frequency shift of QCM and the radioactivity change of ^{125}I labeled antibody. In summary, the limit of detection (LOD) and linear range of the calibration curve of the QCM method were 10 ng/ml and 10 to 1000 ng/ml. The correlation coefficients of HSA

concentration between QCM and ELISA were 0.9913 and 0.9864 for the standards and serum samples, respectively. This report illustrates an investigation of SAMs for the preparation of covalently immobilized antibody biosensors.

2. Surface formation, modification and characterization

QCM chips (16MHz, diameter of quartz: 0.8 cm, diameter of Au: 0.5 cm, Yu-kuei, Taiwan) were cleaned by the soxhlet extraction process using a solution (methanol and acetone 1:1) for 24 hrs. Then, the QCM chips were cleaned with ultra pure ethanol (RDH 32205, Riedel-deHaën), and dried with nitrogen. The QCM chips were immersed into a 0.5 mM 11-mercaptoundecanoic acid (11-MUA, $C_{11}H_{22}O_2S$, 450561, Aldrich) ethanol solution for 8 hours and rinsed with pure ethanol twice. The alkanethiols adsorbed spontaneously from solution onto the Au surface. The functionalized thiol groups were chemisorbed onto the Au surface via the formation of thiolate bonds. After being dried by nitrogen, the surface analysis was performed by X-ray photoelectric spectroscopy (XPS) and Fourier-transformed infrared spectroscopy (FTIR).

2.1 Atomic force microscopy image of QCM ship surface

The QCM chip surface was analyzed by the Atomic force microscopy (AFM). The AFM image was acquired with a Slover PRO (NT-MDT, Russia) atomic force microscopy in ambient pressure. The semi-contact mode was used with a frequency of 0.5 μm/s to scan an area of 10×10 μm². The AFM probe was a golden silicon probe (NSG11, NT-MDT, Russia) with the length, width, thickness, resonant frequency and force constant as 100 mm, 35 μm, 2.0 μm, 255 kHz and 11.5 N/m², respectively.

A rough chip exterior may cause an uneven SAMs surface. To investigate the topology characteristics of the surface, AFM was used to observe the QCM chip surface. In Figure 1, the image of the topographical map taken in the semi-contact mode of a 10×10 μm² zone is shown. Figure 1(a) is a surface image of the QCM chip, and Figure 1(b) shows the three-dimensional structure. This impressive image in Figure 1(b) shows a very clear set of surface roughness with a mean depth of about 1.2 μm. A rough surface may provide the opportunity to increase the reaction surface and the effectiveness antibody immobilization. Most SAMs studies were established on the ideal, well-ordered and smooth single-crystal silicon (100 or 111) wafers primed with a metal adhesion layer (Weng et al., 2004, 2006). On the single-crystal silicon wafers, theoretically, all alkanethiols should be bound onto the SAMs surface as an Au-S-C- structure. Unlike the surface of ideal single-crystal silicon wafers, the rough QCM chip surface may be composed of three types of SAMs structures: alkanethiol bound, attachment by adhesion, and sulfonite-Au bonding. The XPS (S 2p, dialkylsulfide and sulfonite species) indicated that the SAMs deposited onto the QCM surface was non-regular.

2.2 Contact angle measurement

The contact angles (θ) were measured in air using a goniometer (Krüss apparatus). A Milli-Q grade water (Millipore Co., Inc.) was used to contact with the sampling dimension by the sessile drop method. For this measurement, 1 μl droplet was placed slightly on the specimen with the needle of a syringe. The value of θ was determined as the volume of the droplet was slowly increased

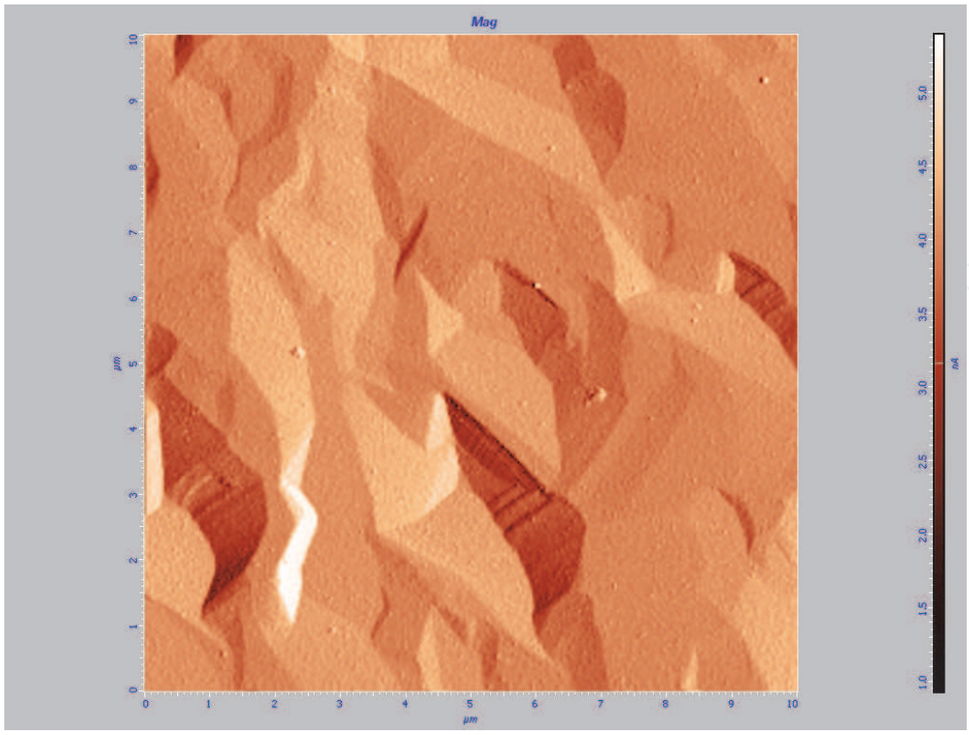

(a)

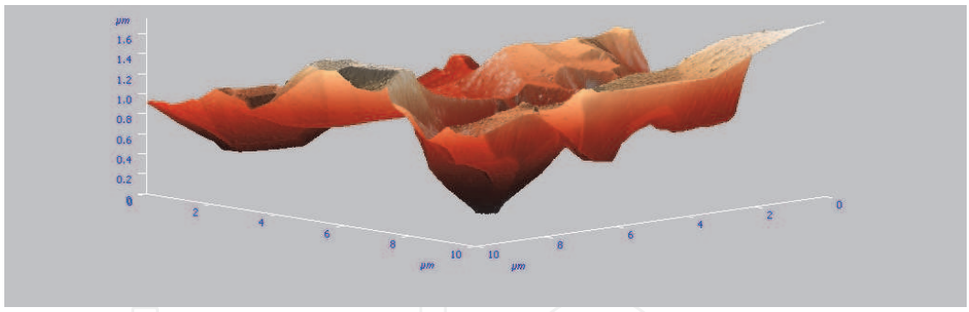

(b)

Fig. 1. AFM images of the Au-covered QCM chip. (a) blank, 10×10 µm, (b) blank, 3D structure. AFM measurements could also be used for measuring the surface roughness of the QCM chip. The mean surface roughness was 1.2 nm.

QCM chip surface	Contact angles (deg)
Au chip	64.1± 2.3
11MUA/Au chip	12.3± 1.6

Table 1. Water Contact Angles Measurement of the SAMs on QCM chip

Contact angles for 11MUA/Au chip using water as probe liquid give advancing contact angles of less than 15°, consistent as a high free energy surface. The SAMs surface with the hydroxyl tail group was hydrophilic. The contact angles agreed well with previous studies (Smith et al., 1992; Lestelius et al., 1997; Laibinis et al. 1991). The above measurements were found unaffected by extending immersion time in the thiol-containing solutions.

2.3 Fourier-transformed infrared reflection-absorption spectroscopy

The infrared (IR) spectroscopy optical benches were acquired with a conventional Fourier-transformed (FT) spectrometer (FTS-175C, Bio-Rad) equipped with a KBr beam splitter and a high-temperature ceramic source. Win-IR, Win-IR Pro (Bio-Rad) and Origin 6.0 (Microcal Software, Inc.) were used for the data acquisition and analysis. The IR spectra were obtained using p-polarized beam incident at a grazing angle of around 80° with respect to the surface normal. The spectra were measured by a liquid-nitrogen cooled, narrow band MCT detector. The spectra were recorded with a resolution of 4 cm^{-1} using about 500 scans and an optical modulation of 15 kHz filter.

The monolayer assembly was routinely characterized with FTIR-RAS upon preparation. Figure 2 shows the FTIR-RAS spectra at 3000~2800 cm^{-1} and 2000~1400 cm^{-1} of the SAMs of carboxylic acid. The peak positions of CH_3 stretching modes were consistent with the presence of a dense crystalline-like phase: r^+, $v_s(CH_3)$ at 2876 cm^{-1}; FR, $v_s(CH_3)$ at 2935 cm^{-1}; r^-, $v_{as}(CH_3)$ at 2963 cm^{-1}. In the spectrum of the SAMs, two absorption peaks at 2920 and 2850 cm^{-1} were assigned to asymmetric (d^-, $v_{as}(CH_2)$) and symmetric (d^+, $v_s(CH_2)$) C-H stretching peaks of the methylene groups [1], respectively (Laibinis et al. 1991). The peak positions of 11-MUA/Au indicated that the frequencies at 1705 cm^{-1} was assigned to residual carboxylic acid stretch, v(C=O) and symmetric carboxylate stretch, $v_s(COO^-)$ (Frey & Corn, 1996).

2.4 X-ray photoelectron spectroscopy measurement

XPS spectra were acquired with a Physical Electronics PHI 1600 ESCA photoelectron spectrometer with a magnesium anode at 400 W and 15 kV-27 mA (Mg K*a* 1253.6 eV, type 10-360 hemispherical analyzer). The specimens were analyzed at an electron take-off angle of 70°, measured with respect to the surface plane. The operating conditions were as follows: pass energy 23.4 eV, base pressure in the chamber below 2×10^{-8} Pa, step size 0.05, total scan number 20, scan range 10 eV (for multiplex scan). The peaks were quantified from high-resolution spectra using a monochromatic Mg X-ray source. Elemental compositions at the surface using C 1s, O 1s and S 2p core level spectra were measured and calculated from XPS peak areas with correction algorithms for atomic sensitivity. The XPS spectra were fitted using Voigt peak profiles and a Shirley background.

The binding structure of the SAMs on the metal surface was monitored by XPS. In the XPS measurements, the variations of O 1s and S 2p with respect to C 1s signal ratios were correlated with the significant presence of chemical species at the SAMs surfaces. The C 1s, O 1s, and S 2p spectra showed the existence of 11-MUA onto the gold-coated QCM chips. The XPS spectra of 11-MUA onto the gold electrode are shown in Figure 3.

In the XPS C 1s spectrum, the peaks of binding energies of core levels at 285.0 eV, 286.9 eV, and 288.8 eV were assigned to the -C-C-, -C-S-, and O=C-O structures, respectively. The C 1s

[1] $v_{s/as}$: symmetric/asymmetric-stretching modes; FR: Fermi resonance.

core-level spectrum of the peak at 286.9 eV and the S 2p spectrum of the peak in 162.0 eV confirmed the Au-S-$(CH_2)_n$- existence. The C 1s core-level spectrum of the peak at 288.8 eV and the O 1s spectrum of the peaks at 532.0 eV and 533.2 eV provided evidence that the terminal groups of SAMs on the QCM chips were the carboxylic acid groups.
In the O 1s spectrum, the peaks of binding energies of O 1s core levels at 532.0 eV and 533.2 eV were assigned to the carboxylic acid group (O*=C-O and O=C-O* for the * marked O, respectively) structure, which was the characteristic group of 11-MUA.

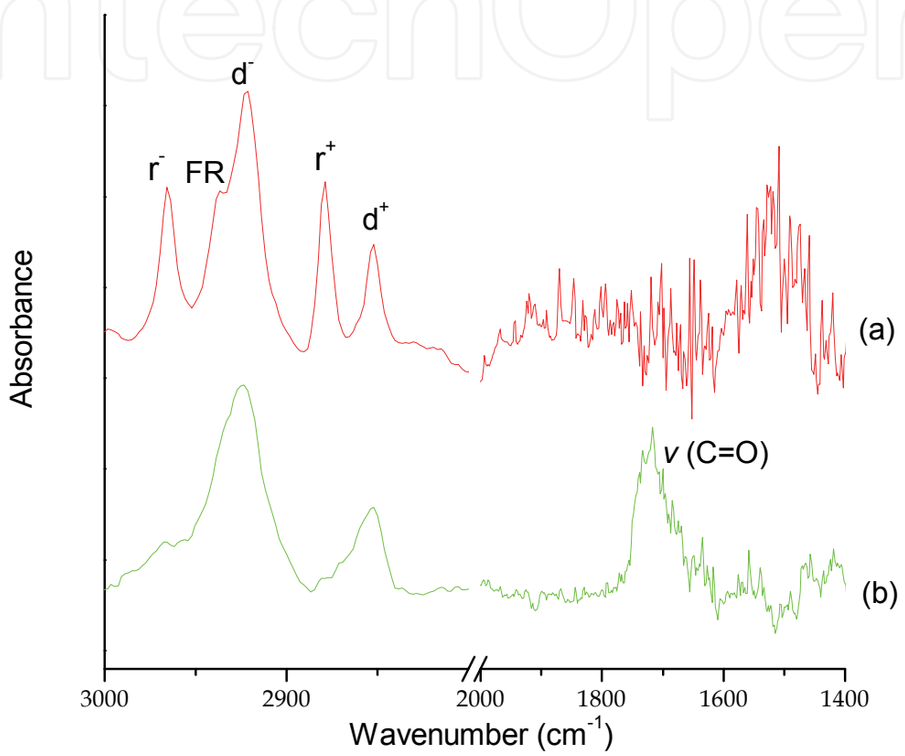

Fig. 2. FTIR-RAS spectra show the frequency regions: 3000 - 2800 and 2000 - 1400 cm^{-1} of the SAMs on the QCM chip. (a) 1-Dodecanethiol (Reference SAMs surface), (b) 11-mercaptoundecanoic acid.

In the S 2p spectrum, the peaks of binding energies of core levels at 162.0 eV, 163.2 eV, and 169.3 eV were assigned to the Au-S-C-, dialkylsulfide, and SO_3-, respectively. The S 2p spectrum inculcated a doublet structure due to the presence of the S $2p_{3/2}$ and S $2p_{1/2}$ peaks using a 2:1 peak area ratio with a 1.2 eV splitting as shown in Figure 3. The peak at 162.0 eV was assigned to sulfur atoms bound to the gold surface as a thiolate species (Castner et al., 1996). The S 2p spectrum of peak at 163.2 eV was assigned to dialkylsulfide as unbound thiol, which may be due to alkanethiols physisorbed as a double layer or adhesion of alkanethiols (Collinson et al., 1992). The S 2p spectrum of peak at 168.5 eV can be attributed to a sulfonite species (SO_3-). The sulfonite species formation was from the rapid oxidation of sulfur on the 11-MUA modified QCM chip surface. Since the sulfur atom was at the bottom of the 11-MUA chains, the XPS signal in detecting S-O was much weaker then that of C with O, which was on the top of the chain. Thus, it was not feasible to fit the S-O peak in the O 1s

spectrum. Although the SAMs structure on the QCM chip was not ideal, it did not affect the antibody immobilization onto the tail group because the EDC and NHS only functioned on the carboxylic acid group.

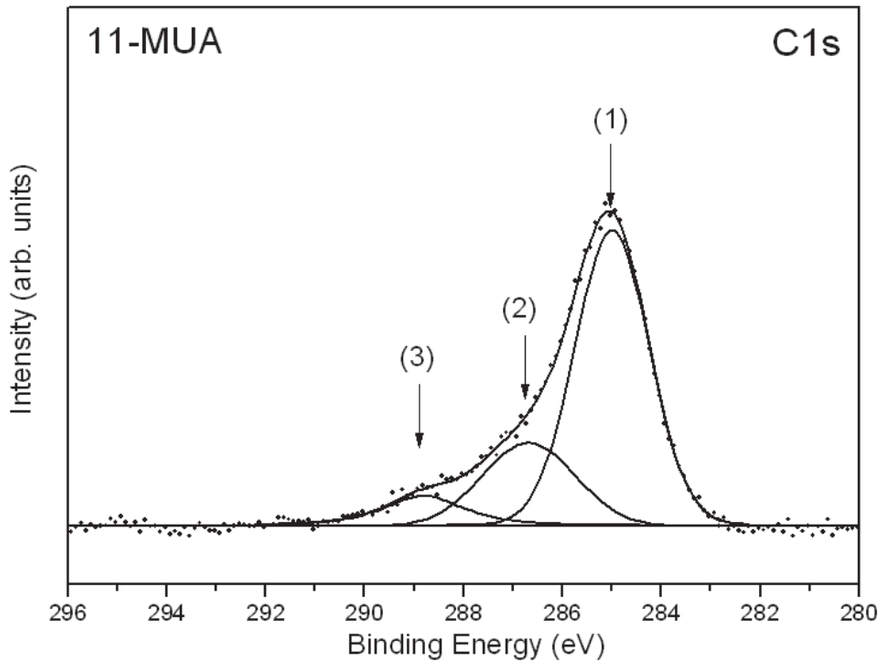

(a)

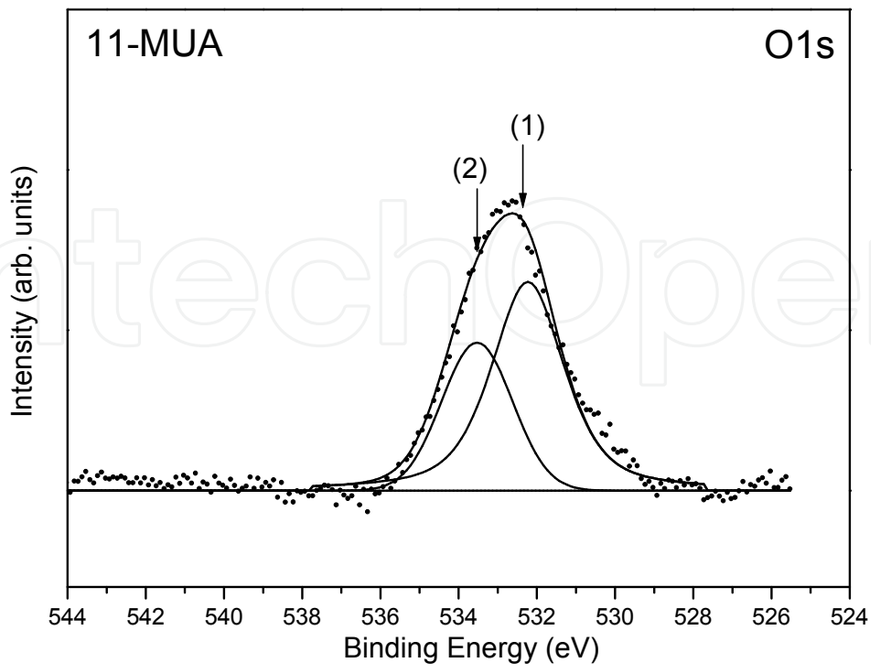

(b)

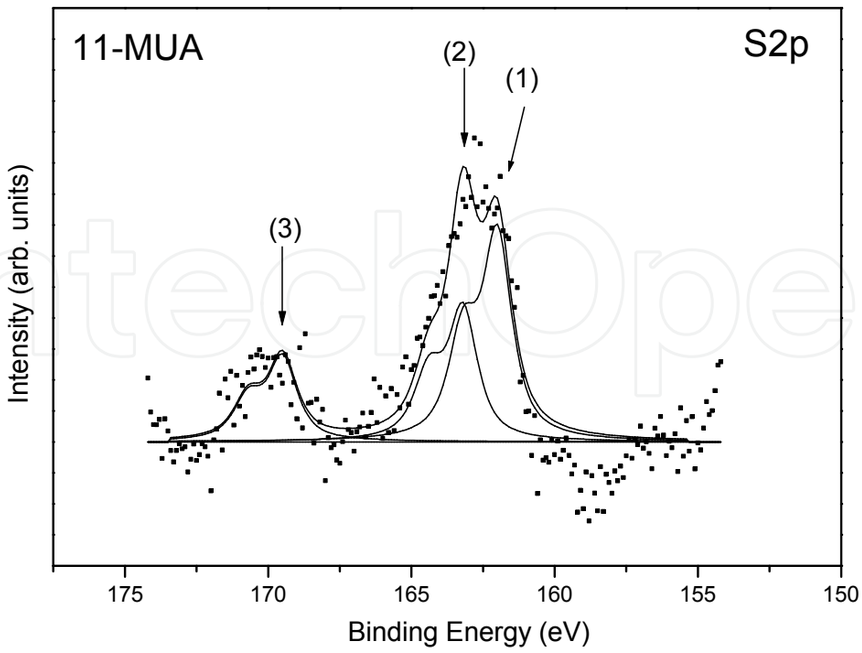

(c)

Fig. 3. XPS spectra of the 11-MUA modified SAMs surface. (a) C 1s, the binding energy at (1) 285.0 eV, (2) 286.9 eV, and (3) 288.8 eV were assigned to the -C-C-, -C-S-, and O=C-O, (b) O 1s, the binding energy at (1) 532.0 eV and (2) 533.2 eV were assigned to the carboxylic acid group, (c) S 2p, the binding energy at (1) 162.0 eV, (2) 163.2 eV, and (3) 169.3 eV were assigned to the Au-S-C-, dialkylsulfide, and SO_3^-, respectively.

2.5 Immobilization of anti-HSA

The labeling procedure was adapted from Chloramine T method. The 2.5 µg anti-HSA was added into sodium phosphate buffer (25 µl, pH= 7.5) with $Na^{125}I$ (0.1 mCi, 2.5 µg/µl). After one minute at room temperature, the reaction was stopped by 25 µl sodium metabisulphite (2.5 µg/µl). The Bio-gel p-60 column was conditioned by sodium phosphate buffer (0.01 M) and NaCl solution (0.15 M, contain 2% BSA) for isolating free iodine from ^{125}I labeled anti-HSA.

In order to immobilize ^{125}I anti-HSA monoclonal antibody, the 11-mercaptoundecanoic acid/Au surface was immersed in the solution containing coupling agents: 75 mM N-ethyl-N'-(3-dimethylaminopropyl) carbodiimide hydrochloride (EDC, E-6383, Sigma) and 15 mM *N*-hydroxysuccinimide (NHS, H-7377, Sigma) at 4 °C for 30 min (van Delden et al., 1997; Kuijpers et al., 2000). Water-soluble EDC and NHS were used to activate O=C-OH (Kang et al., 1993; Tyan et al., 2002) and then the EDC-NHS solution was replaced by a phosphate buffered saline (PBS, URPBS001, UniRegion Bio-Tech), containing 0.2 µg/mL HSA-antibody at 4 °C for 24 hrs. The SAMs chips were thereafter washed by D.I. water and freeze-dried. During the reactions, EDC converted the carboxylic acid group into a reactive intermediate, which was attacked by amines. The radioactivity of each ^{125}I anti-HSA monoclonal antibody immobilized QCM chip was measured by the Scaler cobra II series auto-gamma counting system (Packard, USA, Energy window: 15~75 keV, detection efficiency > 75%, resolution < 34%, detector background <25 cpm).

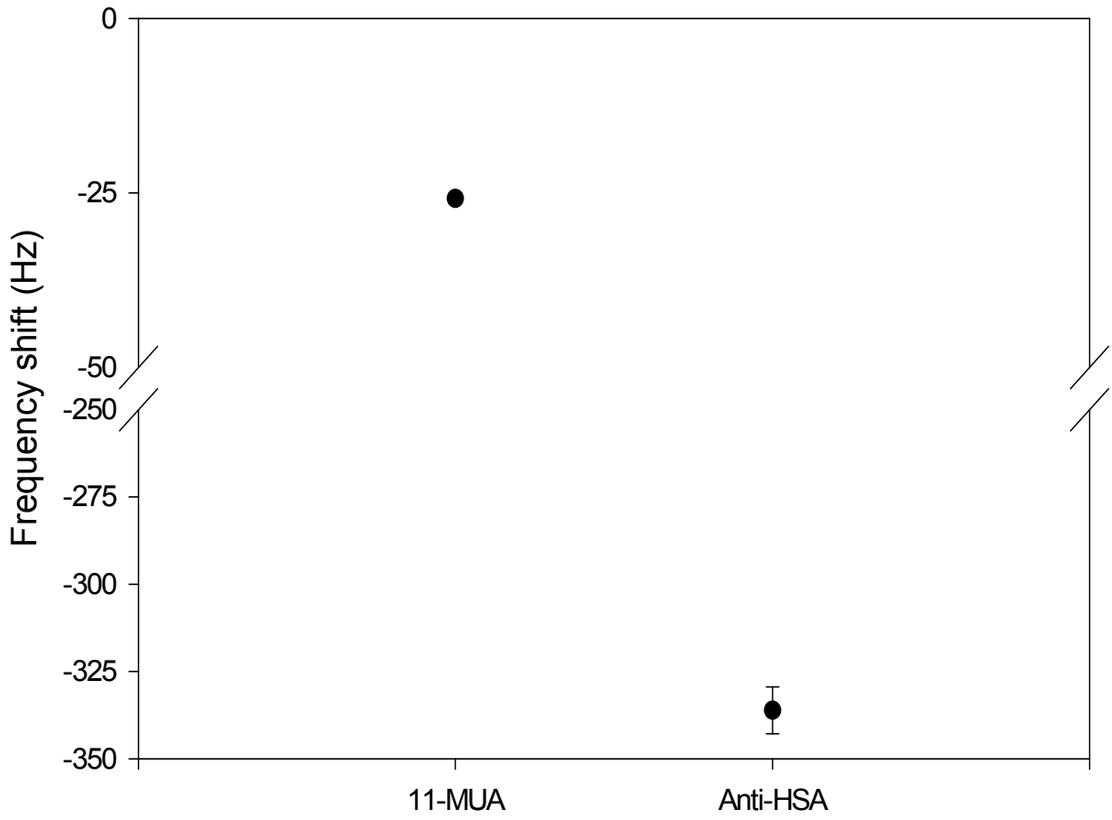

Fig. 4. The oscillation frequency shift of SAMs-QCM chips after 11-MUA and anti-HSA monoclonal antibody immobilization.

The QCM frequency variation after SAMs formation was lowered to around –25.82±4.25 Hz (Figure 4). In this experiment, water-soluble EDC and NHS were used to convert the carboxylic acid of the 11-MUA monolayer to a NHS ester. This reaction activated the 11-MUA-NHS ester monolayer with an aqueous solution of an amine or ammonia, which formed an amide bond with the surface. For the QCM and radioimmunoassay measurements, the frequency variations and count rates were correlated with the data from ^{125}I anti-HSA monoclonal antibody-immobilized SAMs-QCM surface. The QCM frequency decreased after the immobilization of ^{125}I anti-HSA monoclonal antibody (Figure 4). Its average and the coefficient of variations were –336.13±41.50 Hz. The count rate of the radioimmunoassay of ^{125}I anti-HSA monoclonal antibody was 167±18.4 cpm (counts per minute). Thus, the poly-complex between ^{125}I anti-HSA monoclonal antibody and 11-MUA was formed; amino groups in ^{125}I anti-HSA monoclonal antibodies formed complexes with carboxyl groups of 11-MUA. In the QCM measurements, the variations of QCM frequency shift were correlated with the changes of count rates of the radioimmunoassay on the ^{125}I anti-HSA monoclonal antibody immobilized QCM surface. The amount of the ^{125}I anti-HSA monoclonal antibody immobilized onto QCM chips was 59.62±0.47 ng/cm^2. In this study, the surface modification of QCM was analyzed, and the formation of SAMs structure and antibody adsorption were also confirmed.

3. Quantitation of HSA

There are lots of methods for analysis of HSA as Lowry method (Lowry et al., 1951), CBBG-250 (Flores, 1978), enzymatic method (Javed & Waqar, 2001), dye-binding and shift in color method (Gomes et al., 1998), Chemiluminescence technique (Wei et al., 2008), and radioimmunoassay (Catt & Tregear, 1967). The drawbacks of these methods are low sensitivity, narrow linear range, costly, tedious, or protection problem. This experiment of utilizing quartz crystal microbalance provides an alternative method to determine microelement with less test sample and increase the sensitivity. Immumosensors, having the specificity of antibody-antigen (Ab-Ag) affinities and the high sensitivities of various physical transducers, have gained attention for clinical diagnosis (Morgan et al., 1996). Our study combined both techniques of SAMs and QCM for the immumosensor, where a decrease of the resonance frequency is correlated with the mass accumulated on its surface. In this study, the ELISA method was also used for HSA concentration analysis. The feasibility of SAMs-QCM chips can be proofed by the correlation of HSA concentrations measured by the ELISA and QCM methods.

3.1 QCM frequency measurement

The frequency shift of QCM chips was measured by a muti-channel piezoelectric frequency counter with computer signal analysis software (PZ-1001 Immuno-Biosensor System, Universal Sensors Inc., Metairie, LA, U.S.A). For the HSA standard curve and LOD of QCM frequency measurement, the standard solutions with difference concentrations were prepared by dissolving HSA in normal saline and ranged from 5 - 1200 ng/mL. In the QCM frequency measurement of HSA, 10 μL of the HSA standard solutions or serum samples were deposited on the anti-HSA monoclonal antibody immobilized chip. The chips were agitated slowly at room temperature for 10 min, rinsed by D.I. water, and then air-dried.

The QCM instrument was operated in a humidity-controlled cabinet and the humidity was under 50% RH to prevent the moisture interference. The preparation of chips and the tests of serum samples were done under humidity controlled conditions because the high humidity will increase the frequency shift and bias the results. Each concentration was examined six times per chip in a total of six chips. The same procedures were used for the measurement of serum samples. The frequency of the blank was used as a baseline. The frequency of the QCM chip was linearly decreased with the elevation of the HSA concentration. Thus, the amount of negative oscillation frequency shift ($-\triangle F$) was elevated.

The LOD was described as the smallest detectable amount of HSA adsorbed onto the QCM sensor. It used the peak-to-peak value of the noise range (S/N ratio) in the QCM frequency shifts. In this study, the average of S/N ratios of the QCM frequency shift after antibody immobilization were around 1.39, which was over three times of the standard deviation of the background noise (13.72 Hz). Under these criteria, the LOD of this QCM system for HSA detection was around 10 ng/mL and the linear range of the calibration curve of the QCM method was 10 to 1000 ng/ml.

Figure 5 shows the analytic results of the calibration curve, which was plotted with the QCM frequency shift against the actual HSA concentrations. Compared to the actual HSA concentrations, the QCM data was linearized and generated a regression equation as follows: $y=1.3083x-3.4439$ (x-axis, HSA concentration; y-axis, frequency shift; $R^2=0.9913$). It corresponds to the Sauerbrey equation where the frequency shift solely depends on the mass change. In other words, compounds with larger masses will cause more frequency shift than those of smaller masses. In theory, the correlation between the difference of oscillation frequency ($-\triangle F$) and the HSA concentration should be noted as: $C_{(HSA)} = k \cdot (-$

△F)+b and b=0. However, the background noise amplitude of the blank chip also existed. In this study, the b value in the equation was -3.4439. Although the QCM chip was freeze-dried, the background noise amplitude may be due to the process of antibody immobilization through wet graft and thus increase the amplitude of oscillation of the QCM. In our previously study, three types of SAMs linkage materials, 11-MUA, cystamine dihydrochloride and cystamine/glutaraldehyde, were compared through the measurements of frequency change and radioactivity decay to determent the optimal linkage material and conditions for antibody immobilization (Jong et al., 2009). The method sensitivity is the slope of the calibration curve that is obtained by plotting the response against the analyte concentration or mass (Figure 6). Thus, in this study, 11-MUA was selected to prepare the HSA biosensors.

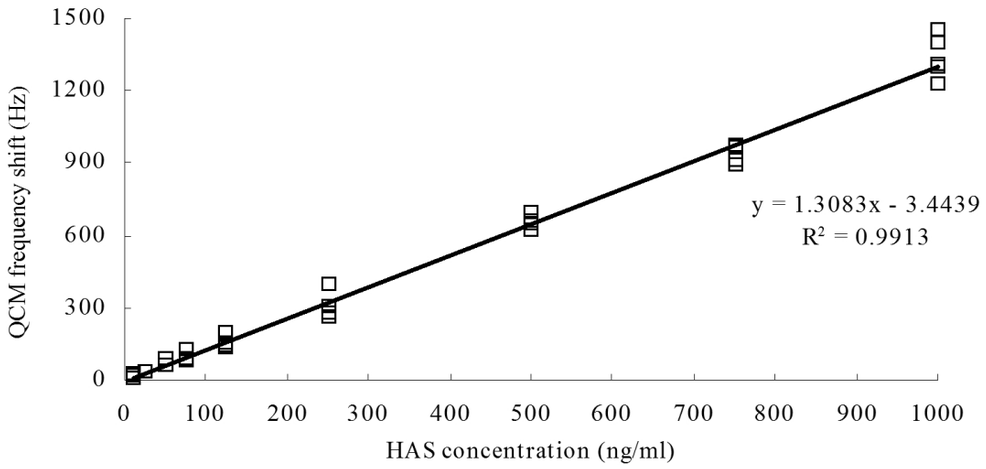

Fig. 5. The calibration curve for HSA standards using anti-HSA monoclonal antibody immobilized QCM chips. The linearity and correlation coefficient were obtained as y=1.3083x-3.4439 and R^2=0.9913.

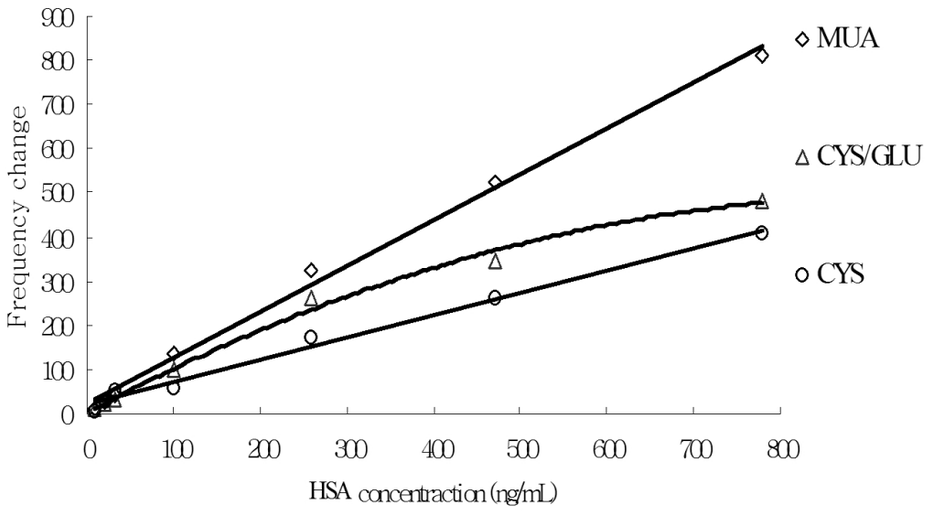

Fig. 6. The slopes of the calibration curve for three types of SAMs linkage materials. The calibration curve of CYS/GLU was a non-linear curve.

3.2 ELISA and QCM measurements of HSA

The HSA concentrations were measured by human albumin ELISA kit (EA2201-1, AssayMax Human Albumin ELISA kit, Assaypro, USA). The HSA standards and serum samples were duplicate counted by the auto-ELISA reader system (Multiskan EX Microplate Photometer, *Thermo* Scientific, USA). The absorbance of the microplate reader was set at a wavelength of 450 nm.

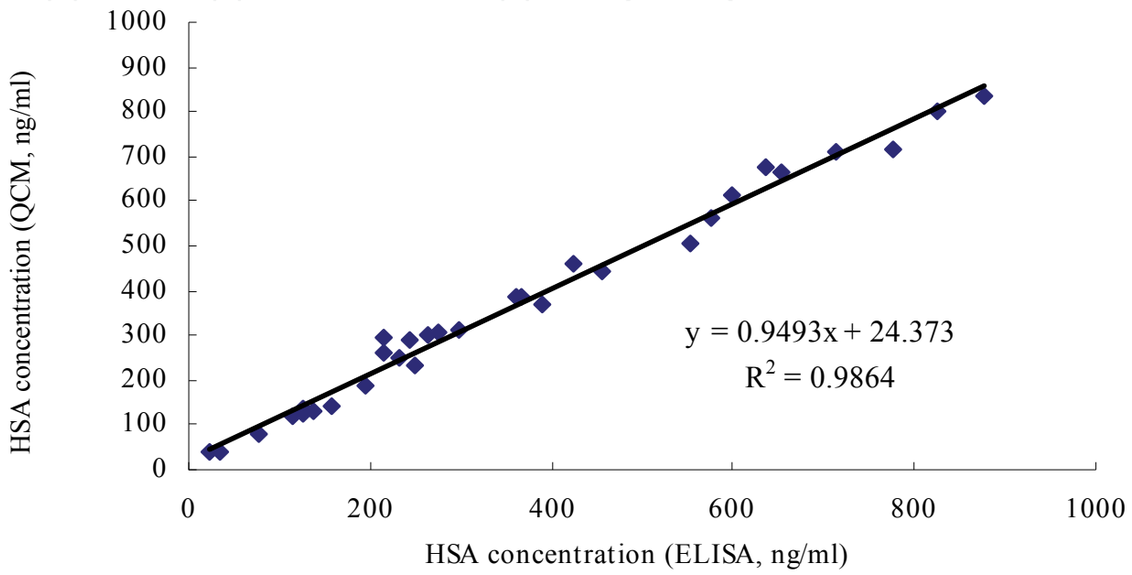

Fig. 7. Detection of HSA in serum samples using QCM chips and ELISA test. The correlation coefficient between the two methods was 0.9864.

The HSA concentrations in serum samples were calculated using the interpolation of the calibration curve and ELISA methods, respectively. Figure 7 shows the correlation of HSA concentrations measured by the QCM and ELISA methods. The linear regression equation for these data is as follows: y=0.9493x+24.373 (x-axis, the concentration measured by ELISA, y-axis, the concentrations obtained by QCM, R^2=0.9864). The variations between the results of QCM frequency shifts and ELISA measurements were acceptable. The experimental results showed an excellent correlation between ELISA and QCM methods for HSA detection. The materials for SAMs-QCM are easy to obtain, and this technique is simple and easy to apply on surface-based diagnostics or biosensors. Thus, the QCM method may provide a reference method for measuring serum HSA in a laboratory and may be more feasible for clinical applications than the standard methods.

4. Conclusions

This study provides an example of the 11-MUA self-assembled monolayer applications of the QCM chip. SAMs formation provides an easy technique to prepare the structure that can be further functionalized with biomolecules to yield bio-recognition surfaces for medical devices. The carboxyl functional thiol monolayer offers an excellent approach to immobilize antibodies for selected sensing of different analytes. The application of SAMs for the immobilization of antibodies onto Au surfaces has a considerable potential in application of

reproducible and reliable biosensors. In this study, the quantization of immobilized antibodies was measured by the shift of QCM frequency and the radioactivity change of ^{125}I labeled antibodies. The LOD of QCM was 10 ng/ml, and the linear range of the calibration curve of QCM method was 10 to 1000 ng/ml. The correlation coefficients between QCM and ELISA were 0.9913 and 0.9864 for HSA in the standards and serum samples, respectively. Compared with ELISA methods, the QCM method was simple and rapid without multiple labeling and purification steps. Our system is different from the conventional approaches in that it operates in the gas phase, not the liquid phase. As a result, there is no waiting time for the frequency to reach stability. In summary, we have presented the modification of the Au interface via 11-MUA SAMs and have proved that the SAMs on Au can be a valid bio-detection chip for HSA concentration analysis by QCM. This assay design of the sensor may develop a potential reference procedure for HSA measurement and has wide applicability in the clinical setting.

5. Acknowledgements

We are thankful to S. Sheldon (ASCP) of the Edmond Medical Center Laboratory (USA) for fruitful discussions. This work was supported by research grants, Q097004 from the Kaohsiung Medical University Research Foundation, NSC96-2321-B-037-006 and NSC97-2320-B-037-012-MY3 from the National Science Council, Taiwan, R.O.C.

6. References

Attli, B.S., Suleman, A.A. (1996). A Piezoelectric Immunosensor for the Detection of Cocaine. *Microchemical Journal*, Vol. 54, No. 2, (August 1996), pp. 174-179, ISSN *0026-265X*.

Ballmer, P.E., McNurlan, M.A., Milne, E., Heys, S.D., Buchan, V., Calder, A.G., Garlick, P.J. (1990). Measurement of albumin synthesis in humans: a new approach employing stable isotopes. *Am J Physiol,* Vol. 259, No. 6, (December 1990), pp. E797-803, ISSN 0193-1849.

Bierbaum, K., Grunze, M., Baski, A.A., Chi, L.F., Schrepp, W., Fuchs, H. (1995). Growth of self-assembled n-alkyltrichlorosilane films on Si(100) investigated by atomic force microscopy. *Langmuir,* Vol. 11, No. 6, (June 1995), pp. 2143-2150, ISSN 0743-7463.

Castner, D.G., Hinds, K., Grainger, D.W. (1996). X-ray Photoelectron Spectroscopy Sulfur 2p Study of Organic Thiol and Disulfide Interactions with Gold Surfaces. *Langmuir,*Vol. 12, No. 2, (October 1996), pp. 5083-5086, ISSN 0743-7463.

Catt, K., Tregear, G.W. (1976). Solid-phase radioimmunoassay in antibody-coated tubes. *Science*, Vol. 158, No. 2, (December 1967), pp. 1570-1572, ISSN 0036-8075.

Chlebowski, R.T., Grosvenor, M.B., Bernhard, N.H., Morales, L.S., Bulcavage, L.M. (1989). Nutritional status, gastrointestinal dysfunction, and survival in patients with AIDS. *Am J Gastroenterol*, Vol. 84, No. 10, (October 1989), pp. 1288-1293, ISSN 0002-9270.

Collinson, M., Bowden, E.F., Tarlov, M.J. (1992). Voltammetry of covalently immobilized cytochrome C on self-assembled monolayer electrodes. *Langmuir*, Vol. 8, No. 2, (May 1992), pp. 1247-1250, ISSN 0743-7463.

Erdelen, C., Haeussling, L., Naumann, R., Ringsdorf, H., Wolf, H., Yang, J., Liley, M., Spinke, J., Knoll, W. (1994). Self-assembled disulfide-functionalized amphiphilic copolymers on gold. *Langmuir*, Vol. 10, No. 4, (April 1994), pp. 1246-1250, ISSN 0743-7463.

Fawcett, N.C., Evans, J.A., Chien, L.C., Flowers, N. (1988). Nucleic acid hybridization setected by Piezoelectric resonance. *Anal Lett*, Vol. 21, No. 7, (July 1988), pp. 1099-1114, ISSN 0003-2719.

Flores, R. (1978). A rapid and reproducible assay for quantitative estimation of proteins using Bromophenol Blue. *Anal Biochem*, Vol. 88, No. 2, (August 1978), pp. 605-611, ISSN 0003-2697.

Frey, B.L., Corn, R.M. (1996). Covalent attachment and derivatization of poly(L-lysine) monolayers on gold surfaces as characterized by polarization-modulation FT-IR spectroscopy. *Anal Chem*, Vol. 68, No. 2, (September 1996), pp. 3187-3193, ISSN *0003-2700*.

Gomes, M.B., Dimetz, T., Luchetti, M.R., Goncalves, M.F., Gazzola, H., Matos, H. (1998). Albumin concentration is underestimated in frozen urine. *Ann Clin Biochem*, Vol. 35, No. 2, (May 1998), pp. 434-435, ISSN 0004-5632.

Gooding, J.J., Hibbert, D.B. (1999). The application of alkanethiol self assembled monolayers to enzyme electrodes. *Trends Anal Chem,* Vol. 18, No. 8, (August 1999), pp. 525-532, ISSN 0165-9936.

Gross, J.L., de Azevedo, M.J., Silveiro, S.P., Canani, L.H., Caramori, M.L., Zelmanovitz, T. (2005). Diabetic nephropathy: diagnosis, prevention, and treatment. *Diabetes Care* , Vol. 28, No. 1, (January 2005), pp. 164-176, ISSN 0149-5992.

Guilbault, G.G. (1983). Determination of formaldehyde with an enzyme-coated piezoelectric crystal detector. *Anal Chem*, Vol. 55, No. 11, (September 1983), pp. 1682-1684, ISSN *0003-2700*.

Guilbault, G.G., Hock, B., Schmid, R.A. (1992). A piezoelectric immunobiosensor for atrazine in drinking water. *Biosensors Bioelectron*, Vol. 7, No. 6, (July 1992), pp. 411-419, ISSN 0956-5663.

Guilbault, G.G., Jordan, J.M., Scheide, E. (1988). Analytical uses of piezoelectric crystals. *Critical Reviews in Analytical Chemistry*, Vol. 19, No. 1, (March 1988), pp. 1-28, ISSN 1040-8347.

Guilbault, G.G., Luong, J.H. (1988). Gas phase biosensors. *J Biotechnol*, Vol. 9, No. 1, (December 1988), pp. 1-9, ISSN 0168-1656.

Himmel, H.J., Weiss, K., Jäger, B., Dannenberger, O., Grunze, M., Woell, C. (1997). Ultrahigh vacuum study on the reactivity of organic surfaces terminated by -OH and -COOH groups prepared by self-assembly of functionalized alkanethiols on Au substrates. *Langmuir*, Vol. 13, No. 19, (September 1997), pp. 4943-4947, ISSN 0743-7463.

Horne, J.C. & Blanchard, G.J. (1998). The role of substrate identity in determining monolayer motional relaxation dynamics. *J Am Chem Soc*, Vol. 120, No. 25, (June 1998), pp. 6336-6344, ISSN 0002-7863.

Javed, M. U., Waqar, S.N. (2001). An enzymatic method for the detection of human serum albumin, *Exp Mol Med*, Vol. 33, No. 2, (June 2001), pp. 103-105, ISSN 1226-3613.

Jong, S.B., Huang, S.L., Lin, C.S., Yang, M.H., Chen, Y.L., Huang, Y.F., Shiea, J.T., Wang, M.C., Tyan, Y.C. (2009). Evaluation the effectiveness of ^{125}I anti-AFP monoclonal antibody on QCM utilizing radioactive measurement. *Chemistry*, Vol. 67, No. 3, (September 2009), pp. 299-307, ISSN 0441-3768.

Joyce, S.A., Thomas, R.C., Houston, J.E., Michalske, T.A., Crooks, R.M. (1992). Mechanical relaxation of organic monolayer films measured by force microscopy. *Phys Rev Let*, Vol. 68, No. 18, (May 1992), pp. 2790-2793, ISSN 0031-9007.

Jung, C., Dannenberger, O., Xu, Y., Buck, M., Grunze, M. (1998). Self-assembled monolayers from organosulfur compounds: A comparison between sulfides, disulfides, and thiols. *Langmuir*, Vol. 14, No. 5, (February 1998), pp. 1103-1107, ISSN 0743-7463.

Kang, I.K., Kwon, B.K., Lee, J.H., Lee, H.B. (1993). Immobilization of proteins on poly(methyl methacrylate) films. *Biomaterials*, Vol. 14, No. 2, (August 1993), pp. 787-792, ISSN 0142-9612.

King, W.H. (1964). Piezoelectric sorption detector. *Anal Chem*, Vol. 36, No. 9, (August 1964), pp. 1735-1739, ISSN *0003-2700*.

Kuijpers, A.J., van Wachem, P.B., van Luyn, M.J., Brouwer, L.A., Engbers, G.H., Krijgsveld, J., Zaat, S.A., Dankert, J., Feijen, J. (2000). In vitro and in vivo evaluation of gelatin-chondroitin sulphate hydrogels for controlled release of antibacterial proteins. *Biomaterials*, Vol. 21, No. 2, (September 2000), pp. 1763-1772, ISSN 0142-9612.

Laibinis, P.E., Nuzzo, R.G., Whitesides, G.M. (1992). The structure of monolayers formed by coadsorption of two n-alkanethiols of different chain lengths on gold and its relation to wetting. *J Phys Chem*, Vol. 96, No. 12, (June 1992), pp. 5097-5105, ISSN 0022-3654.

Laibinis, P.E., Whitesides, G.M. (1992). Self-assembled monolayers of n-alkanethiolates on copper are barrier films that protect the metal against oxidation by air. *J Am Chem Soc*. Vol. 114, No. 23, (November 1992), pp. 9022-9028, ISSN *0002-7863*.

Laibinis, P.E., Whitesides, G.M., Allara, D.L., Tao, Y.T., Parikh, A.N., Nuzzo, R.G. (1991). Comparison of the structures and wetting properties of self-assembled monolayers of n-alkanethiols on the coinage metal surfaces, copper, silver, and gold. *J Am Chem Soc*, Vol. 113, No. 2, (September 1991), pp. 7152-7167, ISSN 0002-7863.

Lestelius, M., Liedberg, B., Tengvall, P. (1997). *In vitro* plasma protein adsorption on ω - functionalized alkanethiolate self-assembled monolayers. *Langmuir*, Vol. 13, No. 2, (October 1997), pp. 5900-5908, ISSN 0743-7463.

Lowry, O.H., Rosebrough, N.J., Farr, A.L., Randall, R.J. (1951). Protein measurement with the Folin phenol reagent. *J Biol Chem*, Vol. 193, No. 2, (November 1951), pp. 265–275, ISSN 0021-9258.

Mariani, G., Strober, W., Keiser, H., Waldmann, T.A. (1976). Pathophysiology of hypoalbuminemia associated with carcinoid tumor. *Cancer*, Vol. 38, No. 2, (August 1976), pp. 854-860, ISSN 1097-0142.

Morgan, C.L., Newman, D.J., Price, C.P. (1996). Immunosensors: technology and opportunities in laboratory medicine. *Clin Chem,* Vol. 42, No. 2, (February 1996), pp. 193-209, ISSN 0009-9147.

Morhard, F., Schumacher, J., Lenenbach, A., Wilhelm, T., Dahint, R., Grunze, M., Everhart, D.S. (1997). Optical diffraction – a new concept for rapid on-line detection of chemical and biochemical analytes. *Proc Electrochem Soc*, Vol. 97, No. 19, (August 1997), pp. 1058-1065, ISSN 0161-6374.

Moshage, H.J., Janssen, J.A., Franssen, J.H., Hafkenscheid, J.C., Yap, S.H. (1987). Study of the molecular mechanism of decreased liver synthesis of albumin in inflammation. *J Clin Invest*, Vol. 79, No. 6, (June 1987), pp. 1635-1641, ISSN 0021-9738.

Muramatsu, H., Tamiya, E., Karube, I. (1988). Computation of equivalent circuit parameters of quartz crystals in contact with liquids and study of liquid properties. *Anal Chem,* Vol. 60, No. 2, (October 1988), pp. 2142-2146, ISSN *0003-2700*.

Nie, L.H., Zhang, X.T., Yao, S.Z. (1992). Determination of quinine in some pharmaceutical preparations using a ring-coated piezoelectric sensor. *J Pharm Biomed Anal*, Vol. 10, No. 2, (July 1992), pp. 529-533, ISSN 0731-7085.

O'Sullivan, C.K., Guilbault, G.G. (1999). Commercial quartz crystal microbalances - theory and applications. *Biosens Bioelectron,* Vol. 14, No. 2, (December 1999), pp. 663-670, ISSN 0956-5663.

Peters, T.J. (1996). *All About Albumin: Biochemistry, Genetics, and Medical Applications.* Academic Press, ISBN 978-0125521109, San Diego, CA, USA.

Phillips, A., Shaper, A.G., Whincup, P.H. (1989). Association between serum albumin and mortality from cardiovascular disease, cancer, and other causes. *Lancet*, Vol. 16, No. 2, (December 1989), pp. 1434-1436, ISSN 0140-6736.

Prinsen, B.H. & de Sain-van der Velden, M.G. (2004). Albumin turnover: experimental approach and its application in health and renal diseases. *Clinica Chimica Acta,* Vol. 347, No. 1-2, (September 2004), pp. 1-14, ISSN 0009-8981.

Rothschild, M.A., Oratz, M., Schreiber, S.S. (1998). Serum albumin. Hepatology, Vol. 8, No. 2, (March 1988), pp. 385-401, ISSN 1665-2681.

Schertel, A., Wöll, C., Grunze, M. (1997). Identification of mono- and bidentate carboxylate surface species on Cu(111) using x-ray absorption spectroscopy. *J Phys IV,* Vol. 7, No. C2, (April 1976), pp. 537-538, ISSN 1155-4339.

Smith, E.L., Alves, C.A., Anderegg, J.W., Porter, M.D., Siperko, L.M. (1992). Deposition of metal overlayers at end-group-functionalized thiolate monolayers adsorbed at gold. 1. Surface and interfacial chemical characterization of deposited copper overlayers at carboxylic acid-terminated structures. *Langmuir*, Vol. 8, No. 2, (November 1992), pp. 2707-2714, ISSN 0743-7463.

Tyan, Y.C., Liao, J.D., Klauser, R., Wu, I.D., Weng, C.C. (2002). Assessment and characterization of degradation effect for the varied degrees of ultra-violet radiation onto the collagen-bonded polypropylene non-woven fabric surfaces. *Biomaterials*, Vol. 23, No. 2, (January 2002), pp. 65-76, ISSN 0142-9612.

van Delden, C.J., Lens, J.P., Kooyman, R.P., Engbers, G.E., Feijen, J. (1997). Heparinization of gas plasma-modified polystyrene surfaces and the interactions of these surfaces with proteins studied with surface plasmon resonance. *Biomaterials*, Vol. 18, No. 2, (June 1997), pp. 845-852, ISSN 0142-9612.

Voinova, M.V., Jonson, M., Kasemo, B. (2002). Missing mass effect in biosensor's QCM applications. *Biosens Bioelectron,* Vol. 17, No. 2, (October 2002), pp. 835-841, ISSN 0956-5663.

Wei, X., Wei, Y., Xing, D., Chen, Q. (2008). A novel chemiluminescence technique for quantitative measurement of low concentration human serum albumin. *Analytical Science,* Vol. 24, No. 2, (January 2008), pp. 115-119, ISSN 1394-2506.

Weng, C.C., Liao, J.D., Wu, Y.T., Wang, M.C., Klauser, R., Grunze, M., Zharnikov, M. (2004). Modification of aliphatic self-assembled monolayers by free-radical-dominant plasma: The role of the plasma composition. *Langmuir*, Vol. 20, No. 2, (October 2004), pp. 10093-10099, ISSN 0743-7463.

Weng, C.C., Liao, J.D., Wu, Y.T., Wang, M.C., Klauser, R., Zharnikov, M. (2006). Modification of monomolecular self-assembled films by nitrogen-oxygen plasma. *J Phys Chem B,* Vol. 110, No. 2, (June 2006), pp. 12523-12529, ISSN 1089-5647.

West, J.B. (1990). *Physiological Basis of Medical Practice.* Williams & Wilkins, ISBN 978-0683089479, Baltimore, MD, USA.

Yan, C., Zharnikov, M., Gölzhäuser, A., Grunze, M. (2000). Preparation and characterization of self-assembled monolayers on indium tin oxide. *Langmuir,* Vol. 16, No. 15, (June 2000), pp. 6208-6215, ISSN 0743-7463.

Biosensors for Health, Environment and Biosecurity
Edited by Prof. Pier Andrea Serra

ISBN 978-953-307-443-6
Hard cover, 540 pages
Publisher InTech
Published online 19, July, 2011
Published in print edition July, 2011

A biosensor is a detecting device that combines a transducer with a biologically sensitive and selective component. Biosensors can measure compounds present in the environment, chemical processes, food and human body at low cost if compared with traditional analytical techniques. This book covers a wide range of aspects and issues related to biosensor technology, bringing together researchers from 16 different countries. The book consists of 24 chapters written by 76 authors and divided in three sections: Biosensors Technology and Materials, Biosensors for Health and Biosensors for Environment and Biosecurity.

How to reference
In order to correctly reference this scholarly work, feel free to copy and paste the following:

Ming-Hui Yang, Shiang-Bin Jong, Tze-Wen Chung, Ying-Fong Huang and Yu-Chang Tyan (2011). Quartz crystal microbalance in clinical application, Biosensors for Health, Environment and Biosecurity, Prof. Pier Andrea Serra (Ed.), ISBN: 978-953-307-443-6, InTech, Available from: http://www.intechopen.com/books/biosensors-for-health-environment-and-biosecurity/quartz-crystal-microbalance-in-clinical-application

INTECH
open science | open minds

InTech Europe
University Campus STeP Ri
Slavka Krautzeka 83/A
51000 Rijeka, Croatia
Phone: +385 (51) 770 447
Fax: +385 (51) 686 166
www.intechopen.com

InTech China
Unit 405, Office Block, Hotel Equatorial Shanghai
No.65, Yan An Road (West), Shanghai, 200040, China
中国上海市延安西路65号上海国际贵都大饭店办公楼405单元
Phone: +86-21-62489820
Fax: +86-21-62489821

© 2011 The Author(s). Licensee IntechOpen. This chapter is distributed under the terms of the Creative Commons Attribution-NonCommercial-ShareAlike-3.0 License, which permits use, distribution and reproduction for non-commercial purposes, provided the original is properly cited and derivative works building on this content are distributed under the same license.

IntechOpen

IntechOpen